Supporting Information for "Numerical Simulation of the Atmospheric Signature of Artificial and Natural Seismic Events"

Léo Martire[1], Quentin Brissaud[2], Voon Hui Lai[2], Raphaël F. Garcia[1], Roland Martin[3], Siddharth Krishnamoorthy[4], Attila Komjathy[4], Alexandre Cadu[1], James A. Cutts[4], Jennifer M. Jackson[2], David Mimoun[1], Michael T. Pauken[4], Anthony Sournac[1]

Contents of this file

1. Texts S1 to S2.
2. Figures S3 to S10.

Introduction This supporting information provides the functional forms of the modelled sources including the values of the scaling factors used, plots comparing the SPECFEM synthetics with a frequency-wavenumber (FK) code, the modelled seismic hammer source time function power spectral density, the atmospheric model used for the earthquakes simulations, earthquakes simulations ground motion synthetics, an illustration of the process of generation of infrasound by seismic surface waves, and a 2D/3D comparison of the amplitudes of synthetic seismic waves.

Text S1. Functional form of the seismic hammer source for the Active Seismic Experiment (ASE). We denote $\mathbf{x} = (x, z)^T$. The spatial reference frame is the usual one, with the x-axis pointing rightward, and the z-axis pointing upward. The vertical point force is under the following form:

$$\mathbf{F}(t, \mathbf{x}) = Ae^{-(\pi f_0 t)^2} \delta_{\mathbf{x}_s}(\mathbf{x}) \begin{pmatrix} 0 \\ -1 \end{pmatrix},$$

where:

- A is an amplification factor,
- f_0 is the dominant frequency of the Gaussian wavelet (chosen as $f_0 = 20$ Hz),
- δ is the Dirac function (source is applied at a single point in space), and
- $\mathbf{x}_s$ is the source location.

We chose $A = 113.437 \times 236 = 2.66711 \times 10^4$ N for ASE-soft, and $A = 113.437$ N for ASE-hard. The "$\times 236$" scaling originates from the up-scaling of synthetics' amplitudes in order to match experimental data amplitude. ASE-hard was not scaled since no particular reference could be found.

Text S2. Functional form of the quake sources for the Passive Seismic Experiment (PSE). We denote $\mathbf{x} = (x, z)^T$. The spatial reference frame is the usual one, with the x-axis pointing rightward, and the z-axis pointing upward. The point moment sources are under the following form:

$$\mathbf{M}(t, \mathbf{x}) = A\left(1 - 2(\pi f_0 t)^2\right) e^{-(\pi f_0 t)^2} \delta_{\mathbf{x}_s}(\mathbf{x}) \begin{pmatrix} M_{xx} & M_{xz} \\ M_{xz} & M_{zz} \end{pmatrix},$$

where:

- A is an amplification factor,
- f_0 is the dominant frequency of the Gaussian derivative wavelet (chosen as $f_0 = 2$ Hz),
- δ is the Dirac function (source is applied at a single point in space),
- $\mathbf{x}_s$ is the source location, and
- M_{xx}, M_{zz}, and M_{xz} are the moment tensor parameters (chosen according to the source mechanism).

For PSE-0, which is a 0° dip fault slip simulation, $M_{xx} = M_{zz} = 0$ and $M_{xz} = -1$. For PSE-45, which is a 45° dip fault slip simulation, $M_{xx} = -M_{zz} = -1$ and $M_{xz} = 0$.

We chose $A = M_0 \times 10^{-3}$ for both cases, with $M_0 = 6.31 \times 10^{12}$ N.m corresponding to a magnitude $M_w = 2.5$ quake ($M_0 = 10^{\frac{3}{2}M_w + 9.05}$ N.m [*Kanamori*, 1977]). The "$\times 10^{-3}$" scaling comes from the fact that we model a 1D fault in a 2D domain: in order to have realistic signal amplitudes, we have to divide by one of the dimensions of the fault. Since $M_0 = \mu AD$ with A the faulting area (μ is the shear modulus, and D the slip displacement), we chose to divide by the typical fault length, which for magnitude 2.5 quakes is $\simeq 10^3$ m [*Westwood et al.*, 2017], hence the scaling.

[1]Institut Supérieur de l'Aéronautique et de l'Espace / SUPAERO, Toulouse University, Toulouse, France.
[2]Seismological Laboratory, California Institute of Technology, Pasadena, CA 91125, USA.
[3]Géosciences Environnement Toulouse, Toulouse University, Toulouse, France.
[4]Jet Propulsion Laboratory, California Institute of Technology, Pasadena, CA 91109, USA.

0094-8276/18/$5.00

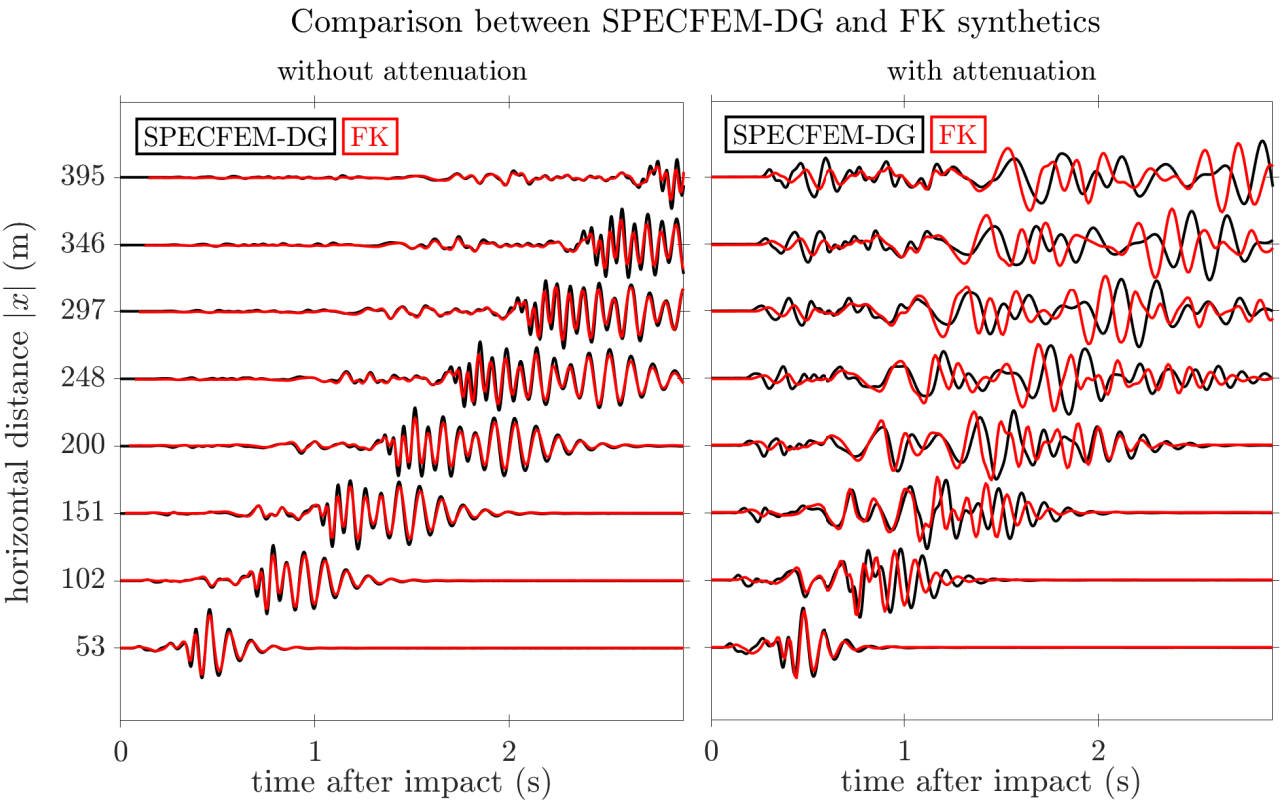

Figure S3. Comparison of ground ($z = 0$ m) vertical velocity synthetics for the active seismic experiment on soft ground (ASE-soft, seismic hammer, see main manuscript) simulations obtained using SPECFEM2D-DG (black) and frequency-wavenumber (FK) method (red). Left: without attenuation. Right: with attenuation. All synthetics are normalised, and filtered using a Butterworth bandpass filter with cut-off frequencies 1 and 20 Hz. Due to the different ways attenuation is implemented in each method, the record sections of synthetics generated with attenuation show a slight phase shift at later arrivals between the synthetics. There is no phase shift between the synthetics for the purely-elastic (without attenuation) case. The phase shift does not affect the overall results and interpretation.

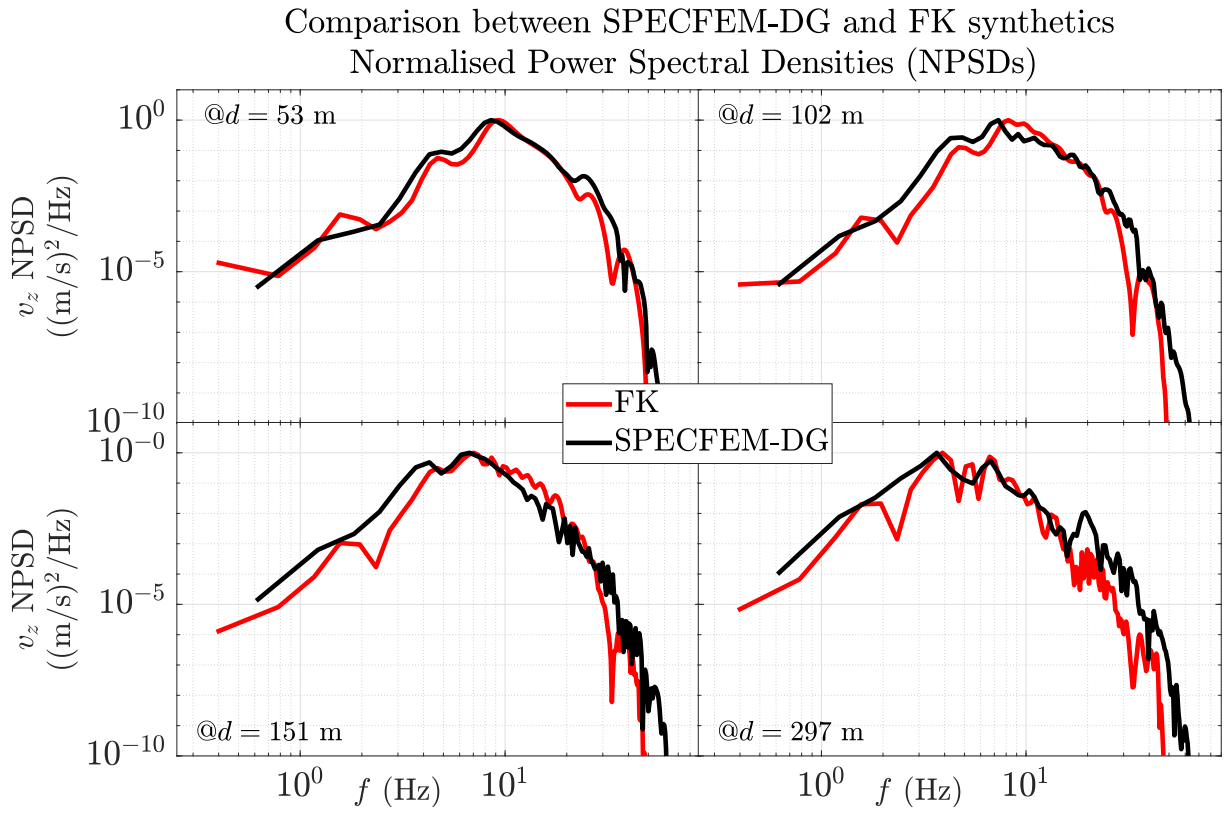

Figure S4. Comparison of the normalised power spectral densities (NPSDs) of the ground ($z = 0$ m) vertical velocity synthetics for the active seismic experiment on soft ground (ASE-soft, seismic hammer, see main manuscript) simulations obtained using SPECFEM2D-DG (black) and frequency-wavenumber (FK) method (red), at different distances from the impact. Attenuation was implemented and used for both. No filter was used beforehand.

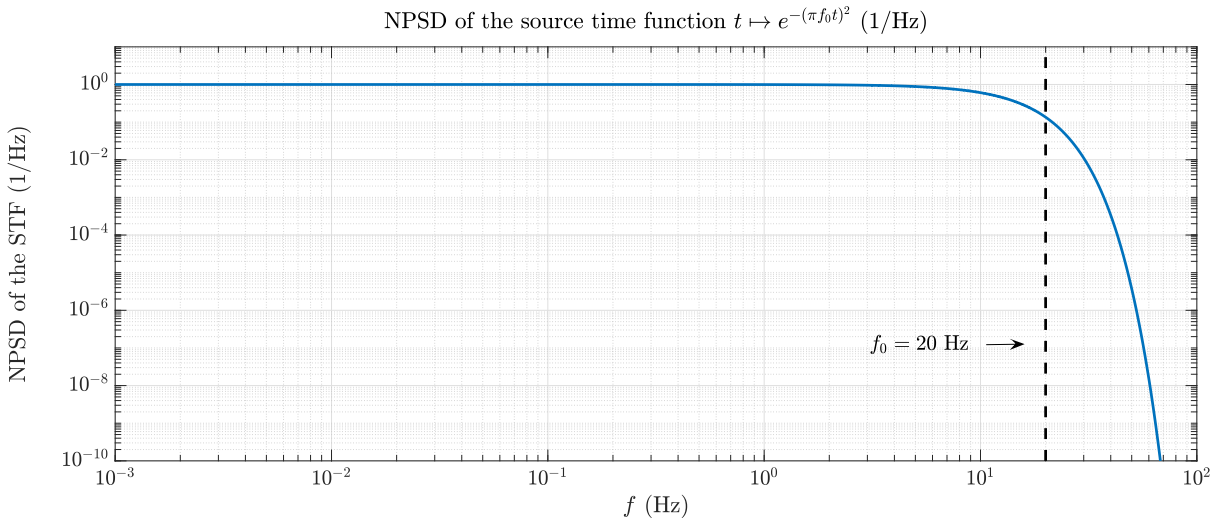

Figure S5. Normalised power spectral density (NPSD) of the time function used for the modelling of the source in the active seismic experiment (ASE-soft and ASE-hard, seismic hammer, see main manuscript) simulations, that is $t \mapsto e^{-(\pi f_0 t)^2}$ (see Text S1). $f_0 = 20$ Hz. Low frequencies are dominant, which could be the cause of the surplus of low frequencies in the synthetics when comparing with data.

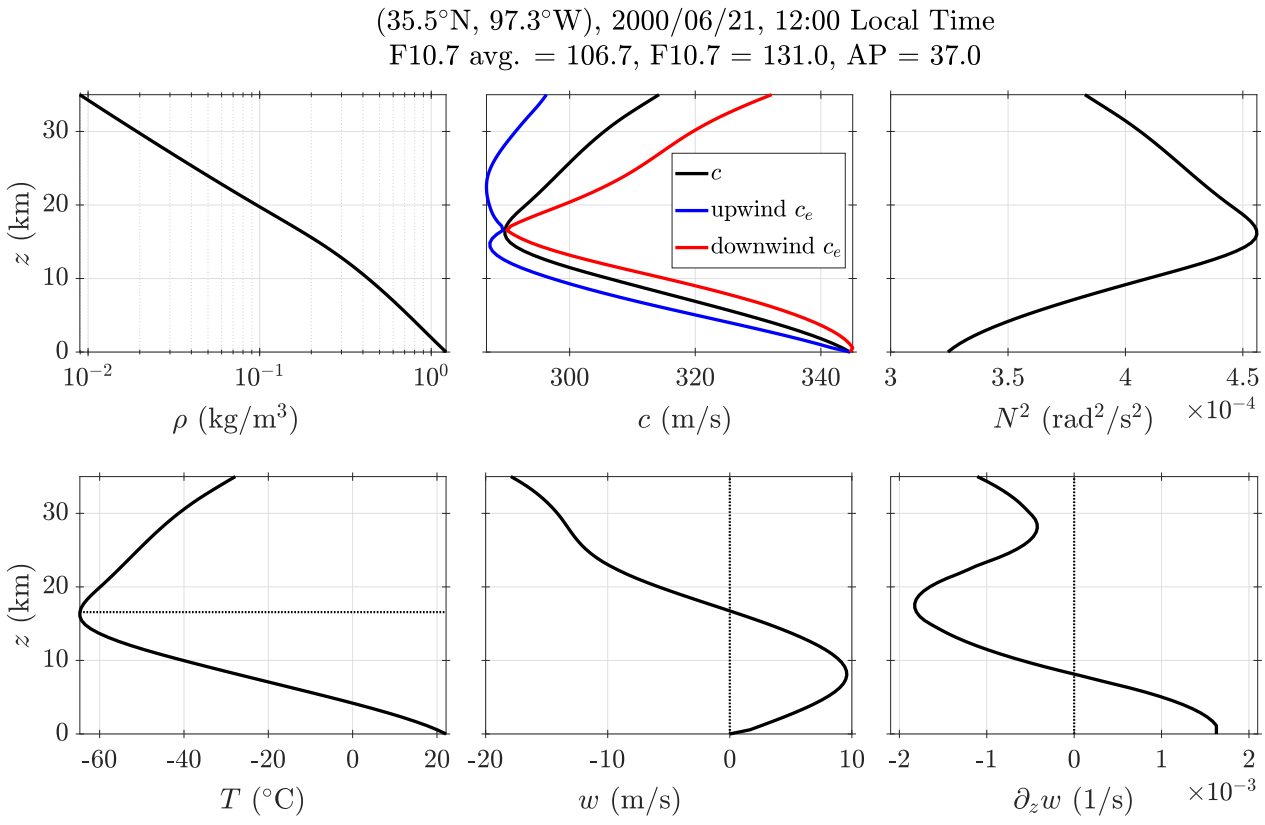

Figure S6. Atmospheric model extracted from MSIS00 and HWM93 and used for the passive seismic experiments (PSE-0 and PSE-45, earthquakes, see main manuscript) simulations. Location is $\simeq$ (35N, 97W), *i.e.* in Oklahoma, on the 21st of June, at local noon. Solar activity parameters (81-day F10.7 flux average, F10.7 flux, and magnetic index AP) used for the call to the model are added in title. From left to right and top to bottom: air density ρ, sound speed c, Brunt-Väisälä frequency N^2, temperature T, horizontal (zonal *i.e.* positive eastward) wind w, and vertical derivative of horizontal wind $\partial_z w$. Recall, no vertical wind component is considered. On the sound speed plot, effective upwind (resp. downwind) sound speed c_e is added as the blue (resp. red) curve. The troposphere limit is added as the horizontal dotted line in the temperature plot. Zero is added as vertical dashed lines in the wind and wind derivative plots.

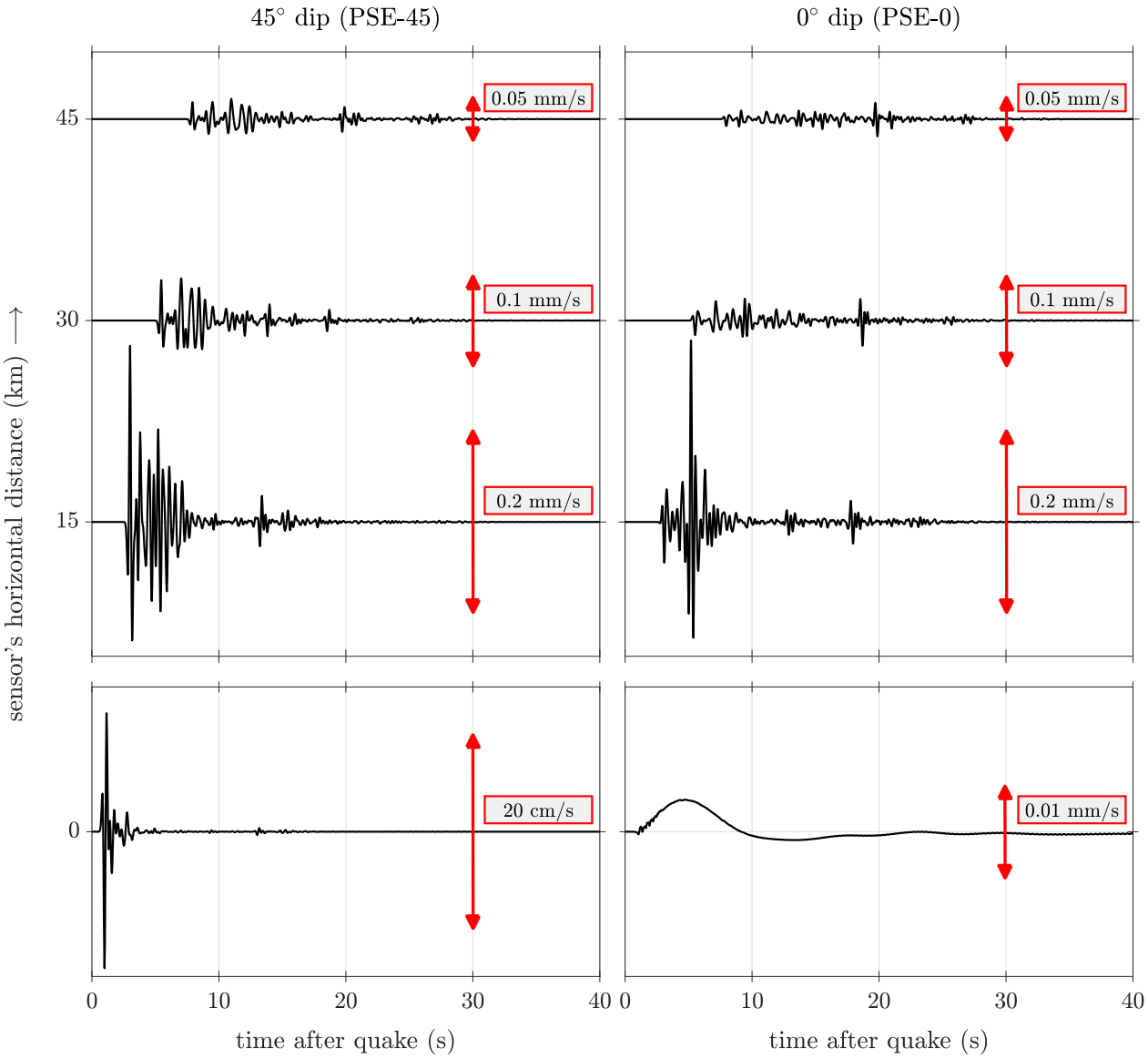

Figure S7. Ground ($z = 0$ m) vertical velocity synthetics for the passive seismic experiments (PSE-0 and PSE-45, earthquakes, see main manuscript) simulations, as function of time, for an horizontal array of stations on ground ($z = 0$ m). Left: 45° dip. Right: 0° dip. Top: away from epicentre, same scale for left and right plots. Bottom: exactly at epicentre, different scales for left and right plots. These synthetics were not filtered. The 45° dip earthquake radiates far more energy upwards than the 0° dip one. Remark that the surface waves' (top) for both sources are of comparable amplitudes (for a given distance) ; yet, in general, the surface waves' amplitudes do depend on the source mechanism [*Tsai and Aki*, 1971, Fig. 6 & 7] [*Aki and Richards*, 2002, Section 7.5]. The amplitude of surface waves decreases with distance due to geometric and intrinsic attenuation.

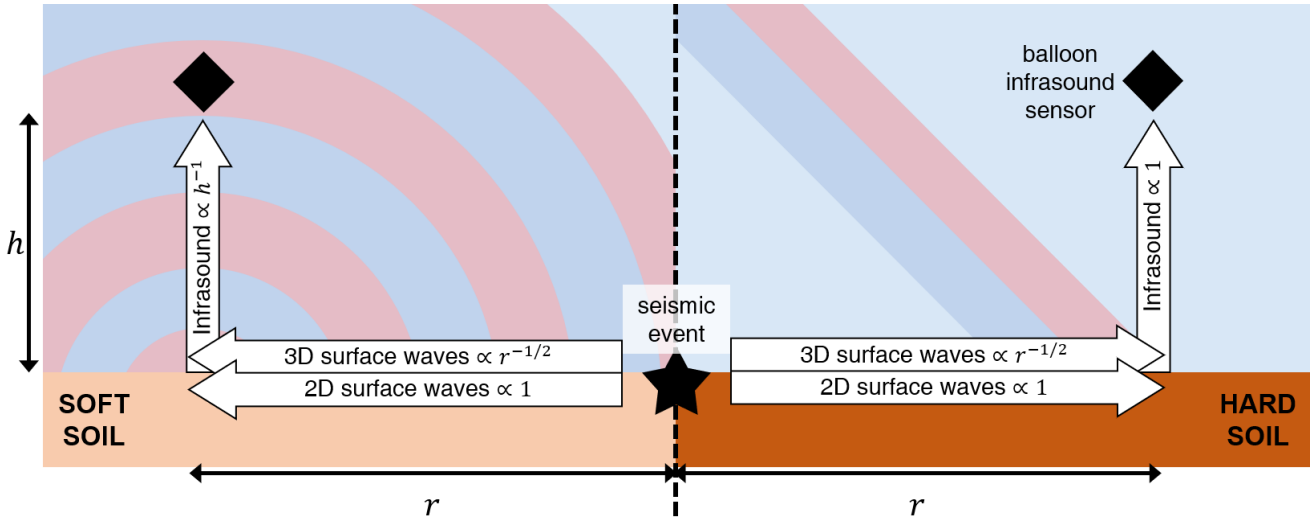

Figure S8. Atmospheric infrasound induced by seismic surface waves depends on 1) said surface waves amplitude and 2) the soil type. The seismic surface waves' geometric attenuation induces a factor $r^{-1/2}$ on amplitude. Viscoelastic (intrinsic) attenuation also plays a significant role. On "soft" soil (see *e.g.* ASE-soft), spherical waves are created (since $v_s \ll c$), while on "hard" soil (see *e.g.* ASE-hard), plane waves are created (since $v_s \gg c$). Thus, the amplitude of infrasound created on soft soil does decrease vertically, while the amplitude of infrasound created on hard soil barely decreases vertically (see also Figure S10).

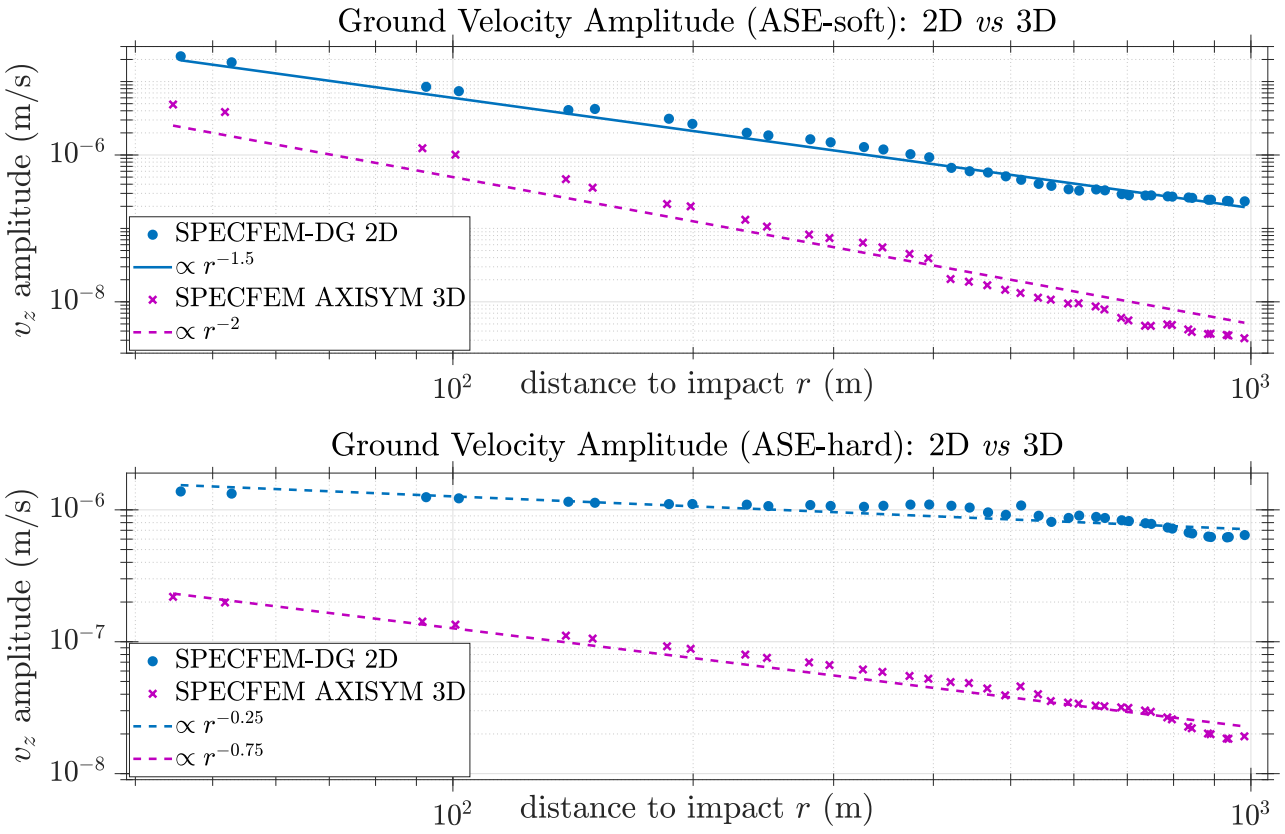

Figure S9. 2D *vs.* 3D propagation. Ground ($z = 0$ m) vertical velocity synthetics' amplitudes for the active seismic experiment on both soils (ASE-soft and ASE-hard, seismic hammer, see main manuscript), as function of distance to the impact. As dots, amplitudes obtained with SPECFEM-DG 2D. As crosses, amplitudes obtained with SPECFEM AXISYM (classic *i.e.* not DG), a simulation tool exploiting axisymmetry to model 3D propagation. Dashed lines highlight trends. The $r^{-1/2}$ factor from 2D to 3D, due to geometric attenuation, appears clearly. *N.B.*: axisymmetric simulations aren't supported yet by the DG extension.

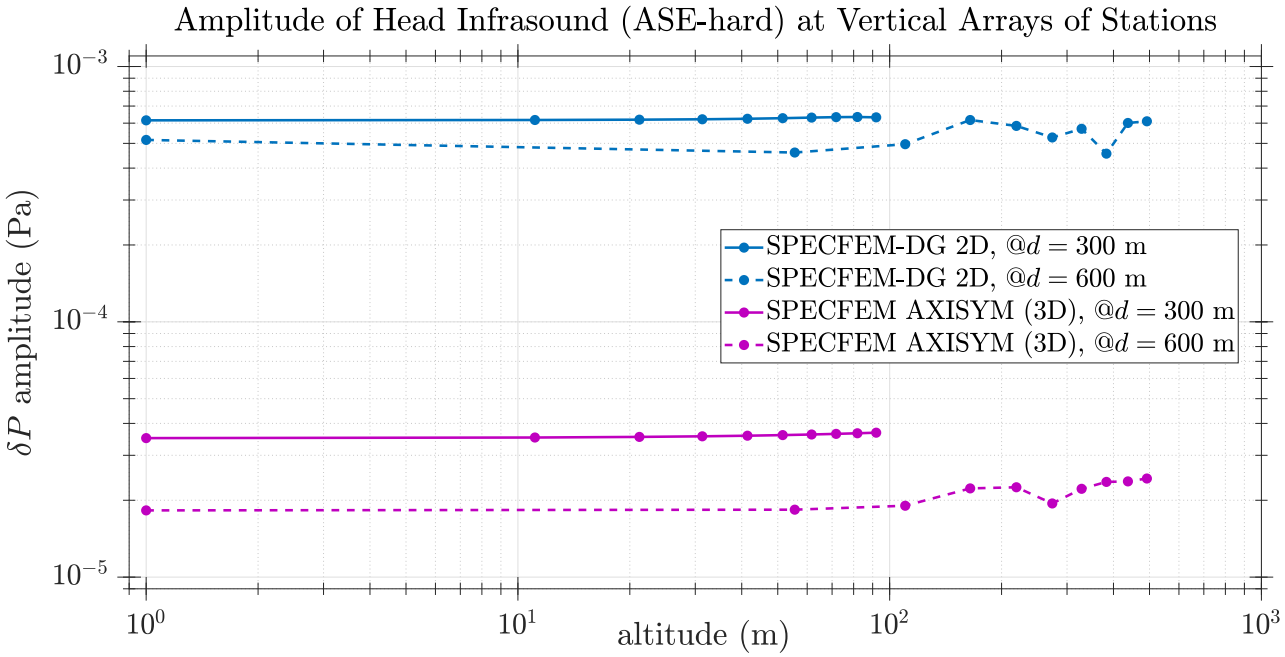

Figure S10. 2D *vs.* 3D propagation. Pressure perturbation synthetics' amplitudes of the head infrasound in the active seismic experiment on hard soil (ASE-hard, seismic hammer, see main manuscript), as function of altitude. In blue, amplitudes obtained with SPECFEM-DG 2D. In purple, amplitudes obtained with SPECFEM AXISYM (classic *i.e.* not DG), a simulation tool exploiting axisymmetry to model 3D propagation. Solid lines are synthetics' amplitude at a vertical array placed at an horizontal distance of 300 m away from the source. Dashed lines are synthetics' amplitude at a vertical array placed 600 m away from the source. For a given horizontal distance, amplitude is always nearly constant with altitude. For a given altitude, amplitude always decreases with horizontal distance, since the generating surface wave's amplitude decreases with horizontal distance (see also Figure S9). *N.B.*: axisymmetric simulations aren't supported yet by the DG extension.